The Journal of Physical Chemistry Letters

pubs.acs.org/JPCL Letter

Gas Phase Synthesis of the Elusive Trisilacyclopropyl Radical (Si_3H_5) via Unimolecular Decomposition of Chemically Activated Doublet Trisilapropyl Radicals (Si_3H_7)

Srinivas Doddipatla, Zhenghai Yang, Aaron M. Thomas, Yue-Lin Chen, Bing-Jian Sun, Agnes H. H. Chang,* Alexander M. Mebel,* and Ralf I. Kaiser*

Cite This: *J. Phys. Chem. Lett.* 2020, 11, 7874−7881 Read Online

ABSTRACT: The gas phase reaction of the simplest silicon-bearing radical silylidyne (SiH; $X^2\Pi$) with disilane (Si_2H_6; X^1A_{1g}) was investigated in a crossed molecular beams machine. Combined with electronic structure calculations, our data reveal the synthesis of the previously elusive trisilacyclopropyl radical (Si_3H_5)—the isovalent counterpart of the cyclopropyl radical (C_3H_5)—along with molecular hydrogen via indirect scattering dynamics through long-lived, acyclic trisilapropyl (i-Si_3H_7) collision complex(es). Possible hydrogen-atom roaming on the doublet surface proceeds to molecular hydrogen loss accompanied by ring closure. The chemical dynamics are quite distinct from the isovalent methylidyne (CH)−ethane (C_2H_6) reaction, which leads to propylene (C_3H_6) radical plus atomic hydrogen but not to cyclopropyl (C_3H_5) radical plus molecular hydrogen. The identification of the trisilacyclopropyl radical (Si_3H_5) opens up preparative pathways for an unusual gas phase chemistry of previously inaccessible ring-strained (inorgano)silicon molecules as a result of single-collision events.

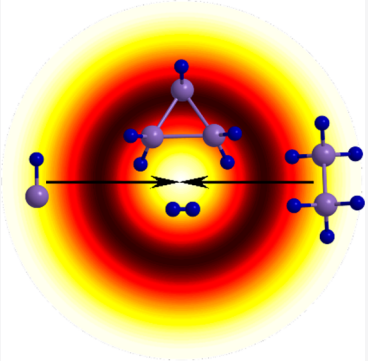

For more than a century, Langmuir's conception of isoelectronicity has been influential in ascertaining modern perceptions of chemical bonding and molecular structure with particular attention dedicated to elucidating the similarities and disparities of the chemistries of carbon and silicon along with the methylidyne (CH) and silylidyne (SiH) radicals.[1,2] The main group 14 elements carbon and silicon are isovalent with four valence electrons each. However, the distinct chemical bonding features of carbon and silicon are evident when comparing the SiC_2H_2 and C_3H_2 potential energy surfaces and the cyclopropyne (c-C_2CH_2) and silacyclopropyne (c-C_2SiH_2) isomers in particular (Scheme 1).[3−5] Singlet cyclopropyne **I** represents a transition state,[5] while silacyclopropyne **II** has been found to be a true local minimum.[3] Consequently, the replacement of a single carbon by an isovalent silicon atom may lead to novel molecules, whose carbon-analogue counterparts do not exist. Thus, (organo)silicon molecules are exploited as benchmarks to understand the resemblances but also distinctions in the chemical bonding and molecular structures compared to their isovalent hydrocarbon counterparts.[6,7]

Scheme 1. Lewis Structures of Cyclopropyne (c-C_2CH_2) and Silacyclopropyne (c-C_2SiH_2)[a]

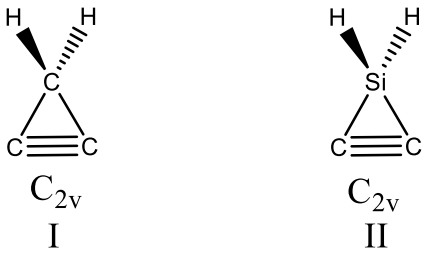

[a]I represents a transition state.

Whereas the chemistries and molecular structures of organosilicon molecules carrying a single silicon atom such as the SiC_2H_n (n = 2−8) families have been explored extensively,[3,8−12] higher homologues in this series, in which *all* carbon atoms are substituted by silicon, are scarce.[6,7,13−16] This is in particular true for the isovalent C_3H_5 and Si_3H_5 systems. The resonantly stabilized, C_{2v} symmetric allyl radical (**III**) represents the global minimum on the C_3H_5 surface with the 1-propenyl (**IV**), 2-propenyl (**V**), and cyclopropyl radicals (**VI**) being higher in energy by 50 to 135 kJmol^{-1} (Scheme 2).[17] The lack of success in isolating *any* free Si_3H_5 radical exposes the complication of silicon to form silicon−silicon

Received: July 24, 2020
Accepted: August 19, 2020
Published: August 19, 2020

   https://dx.doi.org/10.1021/acs.jpclett.0c02281
J. Phys. Chem. Lett. 2020, 11, 7874−7881

Scheme 2. Structures of C_3H_5 Isomers (III−VI)[a]

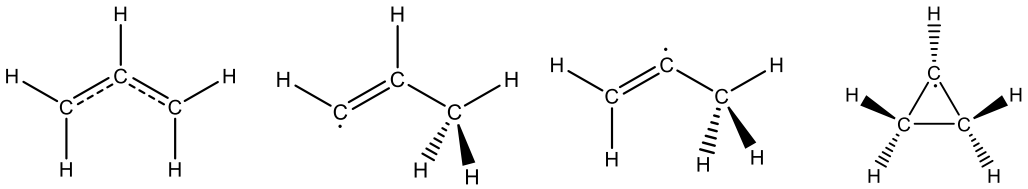

C_{2v}, 0 III | C_s, 100 IV | C_s, 84 V | C_s, 135 VI

[a]Point groups and relative energies (kJ mol^{-1}) with respect to the individual most stable isomer are also given.

double bonds due to the size of the silicon atom that limits an atomic p orbital from approaching sufficiently close to a second silicon atom to form a π bond. However, electronic structure calculations suggest that the Si_3H_5 isomer trisilacyclopropyl (**VII**) and trisilaallyl (**VIII**) should be kinetically stable with **VII** predicted to be energetically favorable by 45 to 70 kJmol^{-1} (Scheme 3).[18,19] Trisilacyclopropyl (**VII**) belongs

Scheme 3. Structures of Si_3H_5 Isomers (VII−IX)[a]

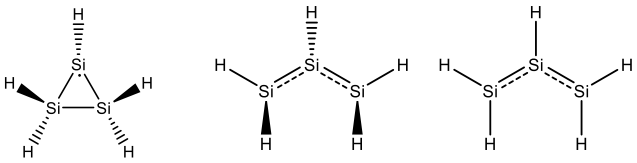

C_s, 0 VII | C_s, 69 VIII | C_{2v}, 65 IX

[a]Point groups and relative energies (kJ mol^{-1}) with respect to the individual most stable isomer are also given.

to the C_s point group and has a $^2A'$ electronic ground state. Whereas the allyl radical (**III**) holds a C_{2v} symmetric structure with all atoms within the plane of symmetry, the C_{2v} symmetric trisilaallyl (**IX**) was predicted to have two imaginary frequencies. Instead, trisilaallyl (**VIII**) favors a C_s symmetric energy minimum and a $^2A''$ electronic ground state with both terminal SiH_2 groups being out-of-plane and highly pyramidal. Frenking et al. reanalyzed the chemical bonding and proposed the cyclic form (**VII**) to be lower in energy than **VIII**, since a stronger σ-bonding in **VII** overcompensates the higher Pauli repulsion.[20] These considerations highlight the striking differences in the molecular structure and bonding of carbon versus silicon (Schemes 2 and 3), thus emphasizing the necessity to prepare higher silicon hydrides to gain fundamental insights into resemblances and distinctions in chemical bonding of carbon versus silicon. This comparison is fundamental to our understanding of chemistry and will affect how we think about the chemical structure of (inorgano)silicon molecules in the future, whose chemical bonding is anticipated to be quite distinct from those of the isovalent carbon counterparts.

Here, we reveal the results of reaction of ground state silylidyne radicals (SiH; $X^2\Pi$) with disilane (Si_2H_6; X^1A_{1g}) under single-collision conditions to prepare for the very first time the previously elusive trisilacyclopropyl radical (Si_3H_5) in the gas phase. Combined with electronic structure calculations, these findings untangle—through the unimolecular decomposition of chemically activated trisilapropyl radical intermediates (Si_3H_7)—an exotic silicon chemistry and unconventional chemical dynamics of silylidyne radicals with disilane, which are fundamentally distinct compared to those of the isovalent carbon-based C_3H_5 system.

The reactive scattering signal was collected at mass-to-charge ratios (m/z) of 91 to 89; very weak ion counts at a level of 10 ± 6% were detected at m/z = 91 and 90 compared to strong scattering signal at m/z = 89. Considering the natural abundances of silicon (^{30}Si (3.10%), ^{29}Si (4.67%), ^{28}Si (92.23%)), this finding suggests the formation of $^{28}Si_3H_5$ (89 amu) along with molecular hydrogen (H_2, 2 amu); signals at m/z = 91 and 90 originate from $^{30}Si^{28}Si_2H_5^+$ and $^{29}Si^{28}Si_2H_5^+$ (Figure 1). Therefore, the laboratory data alone provide compelling evidence on the formation of reaction products

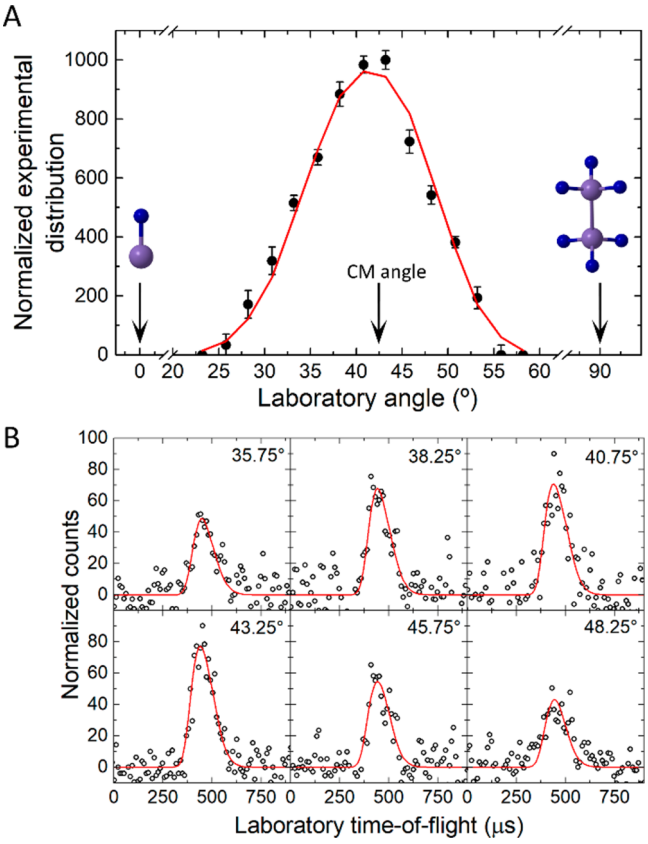

Figure 1. Laboratory angular distribution (A) and time-of-flight spectra (B) recorded at a mass-to-charge ratio of 89 ($Si_3H_5^+$) in the reaction of the ground state silylidyne radical with disilane. The circles define the experimental data, and the red lines represent the fitting based on the best-fit center-of-mass functions as depicted in Figure 2. Here, the CM arrow indicates the center-of-mass angle.

https://dx.doi.org/10.1021/acs.jpclett.0c02281
J. Phys. Chem. Lett. 2020, 11, 7874−7881

with the chemical formula Si_3H_5 plus molecular hydrogen in the reaction of ground state silylidyne radicals with disilane, whereas the atomic hydrogen loss and inherent synthesis of Si_3H_6 isomer(s) are likely closed under our experimental conditions. The laboratory angular distribution obtained at m/z = 89 ($^{28}Si_3H_5^+$) is nearly forward−backward symmetric around the center-of-mass (CM) angle of 42.4 ± 0.6° and spread over 30° (Figure 1). These results propose indirect scattering dynamics involving Si_3H_7 intermediate(s).

The ultimate goal of our study is not only to determine the chemical formula of the reaction product (Si_3H_5) but also to expose the product isomer(s) and the underlying reaction mechanism(s). To gain insights into the reaction dynamics, the laboratory data (TOF spectra, laboratory angular distribution) were transformed into the CM reference frame by employing a forward-convolution routine[21−24] with the product mass combination of 89 amu ($^{28}Si_3H_5$) plus 2 amu (H_2); this procedure yields the translational energy flux distribution $P(E_T)$ and the angular flux distribution $T(\theta)$ (Figure 2). The

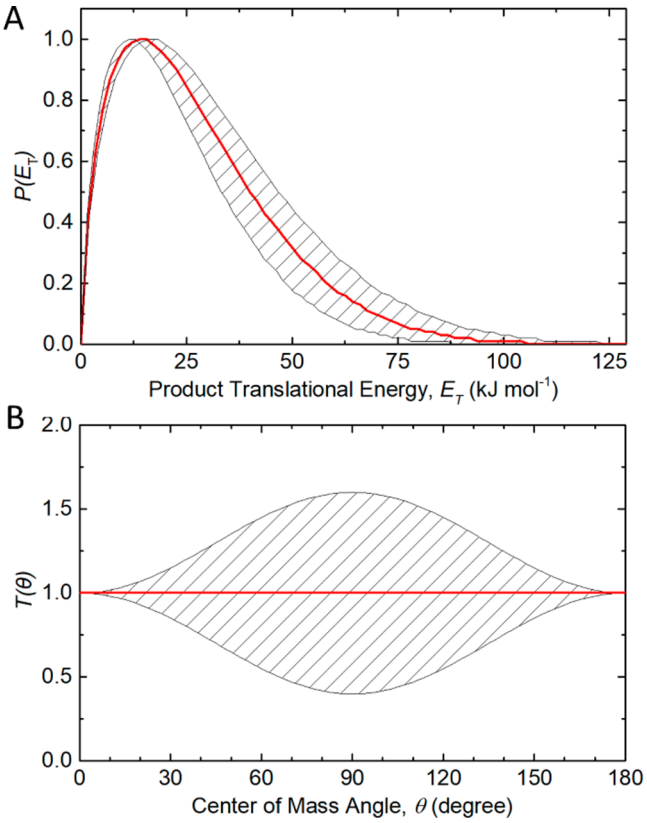

Figure 2. Center-of-mass translational energy flux distribution (A) and angular distribution (B) leading to the formation of the Si_3H_5 molecules plus molecular hydrogen in the reaction of the ground state silylidyne radical with disilane. Shaded areas indicate the acceptable upper and lower error limits of the fits. The red solid lines define the best-fit functions.

translational energy flux distribution, $P(E_T)$, discloses a maximum translational energy (E_{max}) of 104 ± 18 kJ mol^{-1}, which is the sum of collision energy and the reaction energy. Consequently, by subtracting the collision energy from E_{max}, the reaction energy to form Si_3H_5 along with molecular hydrogen is determined to be −68 ± 18 kJ mol^{-1}. Additionally, the $P(E_T)$ reveals a distribution maximum away from zero translational energy suggesting a tight exit transition state of a decomposing intermediate via molecular hydrogen elimination.[25] Further, the CM angular flux distribution $T(\theta)$ depicts a forward−backward symmetric distribution and non-zero intensity from 0° to 180°; this suggests that the reaction proceeds through long lived complex(es).[26,27]

Conceivable Si_3H_5 isomer(s) accessed via the elementary gas phase reaction of ground state silylidyne radicals with disilane can be discovered by comparing the experimentally determined reaction energy (−68 ± 18 kJ mol^{-1}) with the reaction energies obtained from our electronic structure calculations for distinct Si_3H_5 isomers (Figure 3; Theoretical Methods;

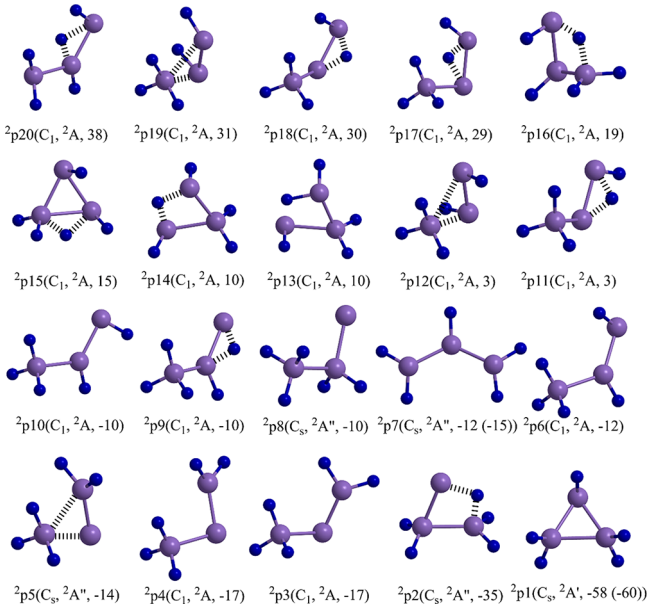

Figure 3. B3LYP/cc-pVTZ computed structures of doublet Si_3H_5 isomers along with their point groups and symmetries of the electronic wave functions. The CCSD(T)/CBS[28]//B3LYP/cc-pVTZ relative energies of products are given in kJ mol^{-1} with respect to the energies of the separated reactants. The CCSD(T)-F12/CBS//B3LYP/cc-pVTZ energies of **p1** and **p7** are in parentheses.

Supporting Information). Among the 27 Si_3H_5 isomers, the reaction energy to prepare the thermodynamically most stable isomer—the trisilacyclopropyl radical (Si_3H_5) (^{2}**p1**)—along with molecular hydrogen of −60 ± 4 kJ mol^{-1} agrees well with the experimentally derived reaction energy. Therefore, we can conclude that at least the trisilacyclopropyl radical (Si_3H_5) represents a product of bimolecular reactions of the silylidyne radical with disilane. Considering our collision energy of 36.0 ± 0.5 kJ mol^{-1}, the Si_3H_5 isomers ^{2}**p2** to ^{2}**p19** might also contribute to the reactive scattering signal, and their presence could be masked by the low energy section of the center-of-mass translational energy distribution (Figure 2). Note that for completeness, we also explored the energetics of the atomic hydrogen loss leading to 20 Si_3H_6 isomers (Figure 4). Even the formation of the thermodynamically most stable trisilacyclopropane isomer (^{1}**p1**) is endoergic by 30 kJ mol^{-1}. We attempted to fit the laboratory data also with a hydrogen loss channel leading to trisilacyclopropane (^{1}**p1**), but the resulting TOFs are too slow and the simulated laboratory angular distribution is too narrow. Therefore, if formed at all, trisilacyclopropane (^{1}**p1**) would represent only a minor fraction of the products. Consequently, in the bimolecular reaction of silylidyne radicals with disilane, at least the

https://dx.doi.org/10.1021/acs.jpclett.0c02281
J. Phys. Chem. Lett. 2020, 11, 7874−7881

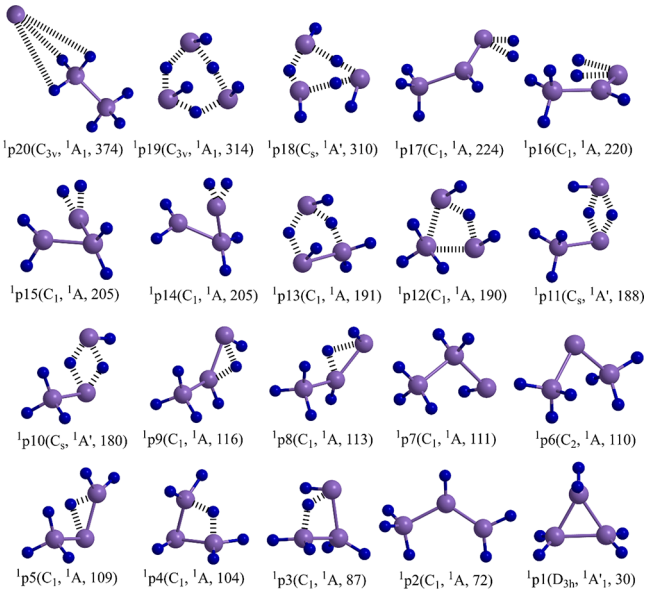

Figure 4. B3LYP/cc-pVTZ computed structures of singlet Si_3H_6 isomers along with their point groups and symmetries of the electronic wave functions. The CCSD(T)/CBS[28]//B3LYP/cc-pVTZ relative energies of the products are given in kJ mol^{-1} with respect to the energies of the separated reactants.

trisilacyclopropyl radical (Si_3H_5) (^{2}**p1**) is formed via molecular hydrogen loss on the doublet surface.

What are the underlying reaction mechanisms leading to the trisilacyclopropyl radical (Si_3H_5) (^{2}**p1**)? Our computations suggest that the reaction commences with a barrierless approach of silylidyne (SiH) to a silicon−hydrogen bond of disilane (Si_2H_6) to form intermediate **i0** residing 57 kJ mol^{-1} below the energy of the separated reactants (Figure 5). This intermediate features one hydrogen atom of the attacked disilane molecule moving to a bridging position between two silicon atoms with the Si−H distances in the bridge being 166 and 167 pm; these distances are longer than regular Si−H bonds of 148−149 pm. The Si−Si bond distance in the Si−H−Si bridge is 261 pm, which is also longer than a regular single Si−Si bond of typically 236 pm. **i0** isomerizes to the *n*-trisilapropyl radical intermediate ($SiH_3SiH_2SiH_2$) **i1** via a barrier of 26 kJ mol^{-1}. During this isomerization, the bridging hydrogen atom shifts to the silicon atom of the former silylidyne reactant, and the formation of the single Si−Si bond is completed. The transition state for this process is very peculiar, as it features two symmetric hydrogen atoms bridging the forming Si−Si bond. Intrinsic reaction coordinate (IRC) calculations in the reverse direction bring the system to an inflection point, representing another symmetric transition state with two bridging hydrogen atoms reflected by the symmetry plane but with a sharpened HSiH angle in the bridge. IRC calculations from this new transition state/inflection point lead to two different enantiomers of **i0** with one of the two distinct hydrogens staying in the bridging position. Intermediate **i1** resides in a deep potential energy well of 183 kJ mol^{-1} relative to the separated reactants and may rearrange to the *i*-trisilapropyl radical ($SiH_3SiHSiH_3$) **i2** via a 1,2-H migration overcoming a 141 kJ mol^{-1} barrier. The molecular hydrogen elimination process from **i1** to the trisilacyclopropyl radical (Si_3H_5) (^{2}**p1**) can proceed via two different mechanisms. In the conventional mechanism, the

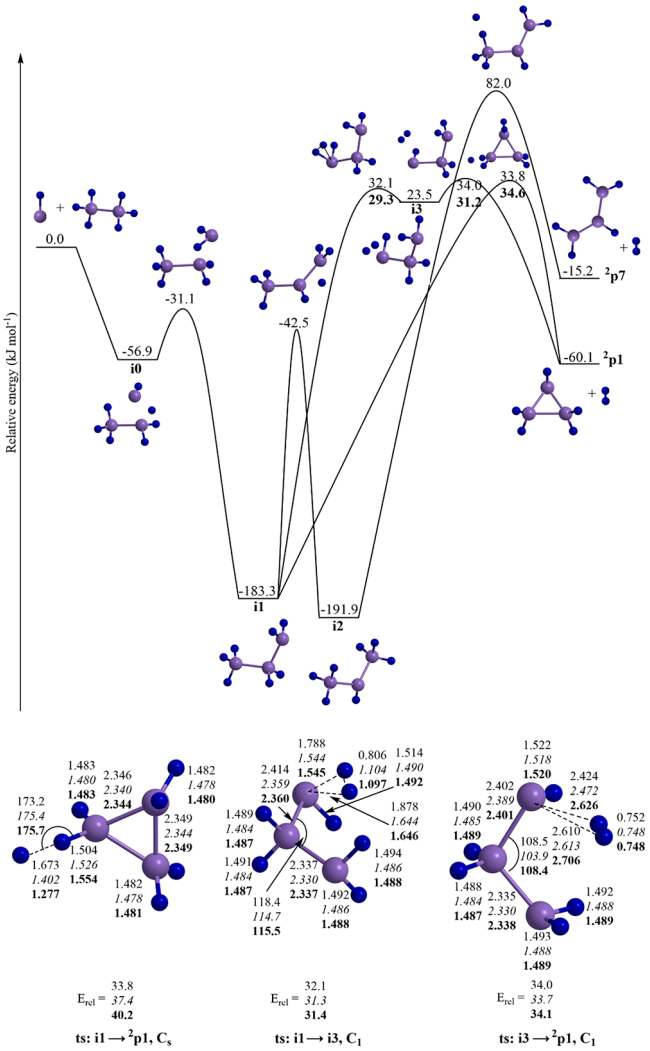

Figure 5. Potential energy diagram of the silylidyne−disilane system leading to the trisilacyclopropyl radical (Si_3H_5) calculated at the CCSD(T)-F12/CBS//B3LYP/cc-pVTZ level of theory. Relative energies are given in kJ mol^{-1} with respect to the reactants. For the critical transition states ts: **i1** → ^{2}**p1**, ts: **i1** → **i3**, and ts: **i3** → ^{2}**p1**, bold numbers show refined relative energies evaluated taking into account core electronic correlation, anharmonicity, and B2PLYPD3 geometry (ts: **i1** → **i3** and ts: **i3** → ^{2}**p1**) corrections (top). Geometries of the critical transition states ts: **i1** → ^{2}**p1**, ts: **i1** → **i3**, and ts: **i3** → ^{2}**p1** optimized at the B3LYP/cc-pVTZ, B2PLYPD3/cc-pVTZ (italic numbers), and CCSD/cc-pVTZ (bold numbers) levels of theory. Relative energies of the transition states with respect to the reactants are given in kJ mol^{-1} as calculated at the CCSD(T)-F12/CBS//B3LYP/cc-pVTZ + ZPE(B3LYP/cc-pVTZ), CCSD(T)-F12/CBS//B2PLYPD3/cc-pVTZ + ZPE(B2PLYPD3/cc-pVTZ) (italic), CCSD(T)-F12/CBS//CCSD/cc-pVTZ + ZPE(B3LYP/cc-pVTZ) (ts: **i1** → ^{2}**p1**) or CCSD(T)-F12/CBS//CCSD/cc-pVTZ + ZPE-(B2PLYPD3/cc-pVTZ) (ts: **i1** → **i3** and ts: **i3** → ^{2}**p1**) (bold) levels of theory, not including core electronic correlation and anharmonicity corrections (bottom).

molecular hydrogen emission takes place from the SiH_3 moiety. At the first step, two Si−H bonds elongate, and a new H−H bond forms in intermediate **i3**, which represents a complex of $SiHSiH_2SiH_2$ with the molecular hydrogen having a stretched H−H bond coordinated to the SiH group. Complex **i3** then decomposes with the hydrogen molecule leaving and a new Si−Si bond formed, leading to the trisilacyclopropyl

https://dx.doi.org/10.1021/acs.jpclett.0c02281
J. Phys. Chem. Lett. 2020, 11, 7874−7881

radical (Si_3H_5) (^{2}**p1**). The relative energies of the transition state connecting **i1** and **i3** as well as **i3** and ^{2}**p1** calculated at the CCSD(T)-F12/CBS/B3LYP/cc-pVTZ level of theory are 32 and 34 kJ mol^{-1}, respectively. In addition to this conventional H_2 elimination pathway, an alternative hydrogen-atom roaming pathway was also found. As illustrated in Figure S1 in the SI, in the roaming pathway, a hydrogen atom is nearly eliminated from **i1** to form a trisilacyclopropane (Si_3H_6) product (^{1}**p1**) but then comes back to abstract another hydrogen atom from a SiH_2 group to produce the trisilacyclopropyl radical (Si_3H_5) (^{2}**p1**). The roaming transition state between **i1** and ^{2}**p1** is located at 34 kJ mol^{-1} above the energy of the separated reactants at the CCSD(T)-F12/CBS/B3LYP/cc-pVTZ level and hence is competitive with the conventional molecular hydrogen loss via intermediate **i3**. For completeness, it shall be mentioned that the dissociation channel of the intermediate **i2** includes a hydrogen-atom loss from one of the SiH_3 groups forming trisilapropene (^{1}**p2**) without an exit barrier. Molecular hydrogen loss from intermediate **i2** via a roaming transition state 82 kJ mol^{-1} above the reactants leads to trisilaallyl (^{2}**p7**). Considering our collision energy of 36 kJ mol^{-1}, neither ^{1}**p2** nor ^{2}**p7** is energetically accessible. According to these computations, the pathways from **i1** to the trisilacyclopropyl radical (Si_3H_5) (^{2}**p1**) are preferred. Notably, our preliminary calculations indicate that there exist other reaction pathways to ^{2}**p7** that are lower in energy than the roaming channel shown in Figure 5. Since these pathways are not directly relevant to the formation of ^{2}**p1** observed experimentally, they will be reviewed in a future, more detailed, publication.

The transition states for the molecular hydrogen loss channel connecting **i1** and **i3**, **i3** and ^{2}**p1**, and **i1** and ^{2}**p1** at the CCSD(T)-F12/CBS//B3LYP/cc-pVTZ level have energies slightly below the collision energy of 36 kJ mol^{-1} of the experiment. We then explored the influence of the level of theory on the energies of the critical transition states. Let us first consider the effect of the theoretical method for geometry optimization (Figure 5). The use of the B2PLYPD3 and CCSD levels for **i1** → ^{2}**p1** results in a significant shortening of the forming H−H bond from 167 to 140 pm and 128 pm and slight elongation of the breaking Si−H bond from 150 to 153 and 155 pm, whereas the remaining geometric parameters remain essentially the same. These changes result in the increase of the single-point relative energy of the for **i1** → ^{2}**p1** transition state computed at the CCSD(T)-F12 level from 34 to 37 and 40 kJ mol^{-1}. The geometric changes are also significant in **i1** → **i3**, where, in going from B3LYP to B2PLYPD3, the breaking Si−H bonds noticeably shorten, while the forming H−H bond strongly elongates. Here, the B2PLYPD3 and CCSD optimized geometries are very similar. In the meantime, the CCSD(T)-F12/CBS single-point energy changes very slightly, from 32 kJ mol^{-1} with the B3LYP optimized geometry to 31 and 31 kJ mol^{-1} with the B2PLYPD3 and CCSD geometries, respectively. For **i3** → ^{2}**p1**, the B3LYP and B2PLYPD3 geometries are similar, whereas the CCSD structure features somewhat longer Si−H distances toward the leaving hydrogen molecule. The relative CCSD(T)-F12/CBS single-point energies with the three different geometries are very close, within 0.5 kJ mol^{-1} from one another. Taking the geometries which give the lowest CCSD(T)-F12/CBS energies of the transition states, we considered further corrections to the CCSD(T)-F12/CBS//B3LYP/cc-pVTZ energy of the roaming **i1** → ^{2}**p1** and to the CCSD(T)-F12/CBS//B2PLYPD3/cc-pVTZ energies of **i1** → **i3** and **i3** → ^{2}**p1**. The core correlation correction is insignificant for **i1** → ^{2}**p1** (+0.03 kJ mol^{-1}) but decreases the relative energies of **i1** → **i3** and **i3** → ^{2}**p1** by 1.4 and 0.8 kJ mol^{-1}, respectively. The anharmonic ZPE corrections are calculated to be −1.8, −1.0, −2.4, and −3.6 kJ mol^{-1} for silylidyne plus disilane, **i1** → ^{2}**p1**, **i1** → **i3**, and **i3** → ^{2}**p1**, respectively, leading to the increase of the relative energy of **i1** → ^{2}**p1** by 0.8 kJ mol^{-1} and the reduction of the relative energies of **i1** → **i3** and **i3** → ^{2}**p1** by 0.6 and 1.8 kJ mol^{-1}. Incorporating all the corrections, for core electronic correlation, anharmonicity, and B2PLYPD3 geometry, we obtain the relative energies of **i1** → ^{2}**p1**, **i1** → **i3**, and **i3** → ^{2}**p1** as 35, 29, and 31 kJ mol^{-1}, respectively. These results indicate that the conventional molecular hydrogen loss pathway via the intermediate **i3** is certainly feasible under the current experimental conditions, whereas the roaming pathway has a slightly higher required energy but is still below the experimental collision energy and hence may contribute, especially considering the possibility of hydrogen-atom tunneling. Considering the complexity of this system, a presentation of a complete surface along with the search for transition states is beyond the scope of this Letter but will be conducted in the future. A more detailed analysis of various dissociation pathways leading to a variety of Si_3H_5 isomers would allow evaluating their relative yields if the reaction follows statistical behavior.

To conclude, the bimolecular gas phase reaction of ground state silylidyne radicals (SiH; $X^2\Pi$) with disilane (Si_2H_6; X^1A_{1g}) depicted indirect scattering dynamics via Si_3H_7 collision complex(es) along with the formation of the previously elusive trisilacyclopropyl radical (Si_3H_5; X^2A') in an overall exoergic reaction (experimental: −68 ± 18 kJ mol^{-1}; computational: −60 ± 4 kJ mol^{-1}). The (roaming mediated) reaction dynamics involve the formation of two key intermediates **i0** and **i1** (*n*-trisilapropyl) on the doublet surface; the endoergic atomic hydrogen loss channels are not open. In strong contrast, the isovalent methylidyne (CH)−ethane (C_2H_6) system solely leads to propylene (C_3H_6; X^1A') plus *atomic* hydrogen, whereas the *molecular* hydrogen loss to the allyl radical (C_3H_5; X^2A_2) and/or the cyclopropyl radical (C_3H_5; X^2A') are closed. On the Si_3H_5 potential energy surface, the C_s symmetric trisilacyclopropyl radical is the most stable isomer, which is in contrast with its carbon analogue, where the C_{2v} symmetric allyl radical (**III**) is the global energy minimum. The stability between the cyclic and allyl radical of Si_3H_5 and C_3H_5 is dictated by σ-bonding and Pauli repulsion. The trisilacyclopropyl radical has a bond length of 232 pm for two equivalent H_2Si−SiH bonds and a bond length of 242 pm for the H_2Si−SiH_2 bond, these are about 87−90 pm longer than C_s symmetric cyclopropyl radical. The dominating σ-bonding prevailing over Pauli repulsion stabilizes the trisilacyclopropyl radical, whereas in its carbon analogue, a stronger Pauli repulsion due to shorter bonds decreases its stability.[20] Therefore, the classical isovalency of the silicon atom and carbon envisages an improper reactivity in this system. This discovery ultimately effects our perception on the chemical reactivity of silicon-based systems and on the thermochemistry, chemical bonding, and reaction mechanism classifying the silylidyne−disilane system as a significant benchmark to a better understanding of the formation of small (inorgano) silicon molecules in the gas phase under single-collision conditions. This contrast of the distinct chemistries of carbon

https://dx.doi.org/10.1021/acs.jpclett.0c02281
J. Phys. Chem. Lett. 2020, 11, 7874−7881

and silicon is fundamental to our understanding of reactivities of silicon and will influence how we explain chemical bonding involving silicon and how we anticipate chemical structure and reactivity in the future.

EXPERIMENTAL METHODS

The elementary reaction of ground state silylidyne radicals (SiH, $X^2\Pi$) with disilane (Si_2H_6; X^1A_{1g}) was explored in a universal crossed molecular beams machine.[29] A pulsed beam of helium seeded silylidyne radicals was produced *in situ* by photodissociation of disilane at 193 nm at 60 Hz in the primary source chamber. The pulsed beam of the silylidyne radicals passed through a skimmer and a four-slit chopper wheel rotating at 120 Hz; the chopper wheel chose a pulse of the silylidyne radical beam with a well-defined peak velocity (v_p) and speed ratio (S) of 1756 ± 14 ms^{-1} and 14.4 ± 1.3, respectively. A pulsed beam of disilane (99.998%, Voltaix) was generated by a second piezoelectric valve operating at 120 Hz, a pulse width of 80 μs, and a peak voltage of −400 V with a backing pressure of 550 Torr. This resulted in a peak velocity and speed ratio of 750 ± 15 ms^{-1} and 7.2 ± 0.4 for the disilane pulse and a collision energy in the intersection region of the scattering chamber of 36.0 ± 0.5 kJ mol^{-1}; the center-of-mass (CM) angle was calculated to be 42.4 ± 0.6°. The 120 Hz repetition rate of both pulsed valves and 60 Hz frequency of the photodissociation laser allows a "laser-on" minus "laser-off" subtraction to eliminate potential background contributions. Any reactively scattered products were then mass filtered after ionization exploiting a quadrupole mass filter and detected by a Daly type TOF detector located in a rotatable, triply differentially pumped ultrahigh vacuum chamber (6×10^{-12} Torr) after electron-impact ionization of the neutral products at an electron energy of 80 eV and an emission current of 2 mA. This detector is rotatable within the plane defined by both supersonic beams allowing the collection of angular-resolved TOF spectra. At each angle, up to 1×10^6 TOF spectra were recorded. The TOF spectra were then integrated and normalized to the intensity of the TOF at the CM angle to obtain the product angular distribution in the laboratory frame.

THEORETICAL METHODS

Geometries of the reactants, products, intermediates, and transition states involved in the silylidyne plus disilane reaction were optimized using the hybrid B3LYP[30,31] density functional theory (DFT) method with Dunning's correlation consistent cc-pVTZ basis set.[32] Vibrational frequencies of all species were computed at the same B3LYP/cc-pVTZ level of theory. For the reactants and critical transition states involved in the pathways for molecular hydrogen loss from Si_3H_7 intermediates, geometry optimization was also carried out at the doubly hybrid DFT B2PLYPD3/cc-pVTZ level of theory[33,34] including Grimme's dispersion correction[35] and using the coupled clusters CCSD/cc-pVTZ approach.[36−39] For the B2PLYPD3/cc-pVTZ optimized structures, vibrational frequencies were recalculated using the same method. Single-point energies were then refined at the explicitly correlated coupled clusters CCSD(T)-F12 level[40,41] with single and double excitations and perturbative treatment of triple excitations. The CCSD(T)-F12 calculations were carried out with the cc-pVTZ-f12 and cc-pVQZ-f12 basis sets,[32,42] and the energies were then extrapolated to the complete basis set (CBS) limit using the following expression:[43] $E_{CBS} = E_{cc\text{-}pVQZ\text{-}f12} + (E_{cc\text{-}pVQZ\text{-}f12} - E_{cc\text{-}pVTZ\text{-}f12}) * 0.69377$. For the reactants and critical transition states, the CCSD(T)-F12/CBS energies were calculated not only for B3LYP but also for B2PLYPD3 and CCSD optimized geometries. For these species, the energies were further refined by taking into account the core electron correlation effects via CCSD(T)-F12 calculations with the cc-pCVTZ-f12 and cc-pCVQZ-f12 basis sets[44] extrapolated to CBS limit, which included all core electrons except 1s electrons of Si atoms in the correlation treatment. Finally, anharmonicity corrections to zero-point vibrational energies were evaluated through calculations of anharmonic frequencies at the B3LYP/cc-pVTZ level of theory using vibrational perturbation theory to the second order (VPT2).[45] The B3LYP and B2PLYPD3 calculations, CCSD geometry optimizations, and VPT2 computations of anharmonic frequencies were performed using the GAUSSIAN 09 package,[46] whereas the CCSD(T)-F12 calculations were carried out employing MOLPRO 2010.[42]

ASSOCIATED CONTENT

Supporting Information

The Supporting Information is available free of charge at https://pubs.acs.org/doi/10.1021/acs.jpclett.0c02281.

Profile of the potential energy surface for the roaming pathway connecting intermediate **i1** with the **p1** product of the molecular hydrogen loss obtained via intrinsic reaction coordinate (IRC) calculations for the corresponding transition state at the B3LYP/6-311G** level of theory followed by geometry optimization of the final IRC structures, optimized Cartesian coordinates (Å), and vibrational frequencies (cm^{-1}) of reactants, H and H_2 dissociation products, intermediates, and transition states involved in the formation of ^{2}**p1** and ^{2}**p7** products from the silylidyne radical (SiH) + disilane (Si_2H_6) reaction (PDF)

AUTHOR INFORMATION

Corresponding Authors

Ralf I. Kaiser − *Department of Chemistry, University of Hawai'i at Manoa, Honolulu, Hawaii 96822, United States;* orcid.org/0000-0002-7233-7206; Email: ralfk@hawaii.edu

Agnes H. H. Chang − *Department of Chemistry, National Dong Hwa University, Shoufeng, Hualien 974, Taiwan;* Email: hhchang@mail.ndhu.edu.tw

Alexander M. Mebel − *Department of Chemistry and Biochemistry, Florida International University, Miami, Florida 33199, United States;* orcid.org/0000-0002-7233-3133; Email: mebela@fiu.edu

Authors

Srinivas Doddipatla − *Department of Chemistry, University of Hawai'i at Manoa, Honolulu, Hawaii 96822, United States*

Zhenghai Yang − *Department of Chemistry, University of Hawai'i at Manoa, Honolulu, Hawaii 96822, United States*

Aaron M. Thomas − *Department of Chemistry, University of Hawai'i at Manoa, Honolulu, Hawaii 96822, United States;* orcid.org/0000-0001-8540-9523

Yue-Lin Chen − *Department of Chemistry, National Dong Hwa University, Shoufeng, Hualien 974, Taiwan*

Bing-Jian Sun − *Department of Chemistry, National Dong Hwa University, Shoufeng, Hualien 974, Taiwan*

Complete contact information is available at:

https://dx.doi.org/10.1021/acs.jpclett.0c02281
J. Phys. Chem. Lett. 2020, 11, 7874−7881

https://pubs.acs.org/10.1021/acs.jpclett.0c02281

Notes

The authors declare no competing financial interest.

■ ACKNOWLEDGMENTS

The Hawaii group thanks the National Science Foundation (NSF) for support under award CHE-1360658. Computer resources at the National Center for High-Performance Computing of Taiwan were utilized in the calculations.

■ REFERENCES

(1) Langmuir, I. The Arrangement of Electrons in Atoms and Molecules. *J. Am. Chem. Soc.* **1919**, *41*, 868−934.

(2) Langmuir, I. Isomorphism, Isostbrism and Covalence. *J. Am. Chem. Soc.* **1919**, *41*, 1543−1559.

(3) Kaiser, R. I.; Krishtal, S. P.; Mebel, A. M.; Kostko, O.; Ahmed, M. An Experimental and Theoretical Study of the Ionization Energies of SiC_2H_x (X = 0, 1, 2) Isomers. *Astrophys. J.* **2012**, *761*, 178.

(4) Maksyutenko, P.; Zhang, F.; Gu, X.; Kaiser, R. I. A Crossed Molecular Beam Study on the Reaction of Methylidyne Radicals [CH($X^2\Pi$)] with Acetylene [C_2H_2($X1\Sigma_g^+$)]—Competing C_3H_2 + H And C_3H+H_2 Channels. *Phys. Chem. Chem. Phys.* **2011**, *13*, 240−252.

(5) Saxe, P.; Schaefer, H. F., III Can Cyclopropyne Really be Made? *J. Am. Chem. Soc.* **1980**, *102*, 3239−3240.

(6) Kosa, M.; Karni, M.; Apeloig, Y. Trisilaallene and the Relative Stability of Si_3H_4 Isomers. *J. Chem. Theory Comput.* **2006**, *2*, 956−964.

(7) Gordon, M. S.; Bartol, D. Molecular and Electronic Structure of Si_3H_6. *J. Am. Chem. Soc.* **1987**, *109*, 5948−5950.

(8) Thiel, W.; Voityuk, A. A. Extension of MNDO to d orbitals: Parameters and Results for Silicon. *J. Mol. Struct.: THEOCHEM* **1994**, *313*, 141−154.

(9) Antoniotti, P.; Canepa, C.; Operti, L.; Rabezzana, R.; Tonachini, G.; Vaglio, G. A. Experimental and Theoretical Study of the Formation of Silicon-Carbon Ion Species in Gaseous Silane/Ethene Mixtures. *J. Phys. Chem. A* **1999**, *103*, 10945−10954.

(10) Coolidge, M. B.; Hrovat, D. A.; Borden, W. T. Ab Initio Calculations on Silicon Analogues of the Allyl Radical. *J. Am. Chem. Soc.* **1992**, *114*, 2354−2359.

(11) Kaiser, R. I.; Gu, X. Chemical Dynamics of the Formation of the Ethynylsilylidyne radical (SiCCH($X^2\Pi$) in the Crossed Beam Reaction of Ground State Silicon Atoms (Si(^{3}P) with acetylene (C_2H_2($X\ 1\Sigma_g^+$)). *J. Chem. Phys.* **2009**, *131*, 104311.

(12) Parker, D. S. N.; Wilson, A. V.; Kaiser, R. I.; Mayhall, N. J.; Head-Gordon, M.; Tielens, A. G. G. M. On the Formation of Silacyclopropenylidene (C-SiC_2H_2) and its Role in the Organosilicon Chemistry in the Interstellar Medium. *Astrophys. J.* **2013**, *770*, 33.

(13) Ishida, S.; Iwamoto, T.; Kabuto, C.; Kira, M. A Stable Silicon-Based Allene Analogue with a Formally sp0-Hybridized Silicon Atom. *Nature* **2003**, *421*, 725−727.

(14) Tanaka, H.; Inoue, S.; Ichinohe, M.; Driess, M.; Sekiguchi, A. Synthesis and Striking Reactivity of an Isolable Tetrasilyl-Substituted Trisilaallene. *Organometallics* **2011**, *30*, 3475−3478.

(15) Veszprémi, T.; Petrov, K.; Nguyen, C. T. From Silaallene to Cyclotrisilanylidene. *Organometallics* **2006**, *25*, 1480−1484.

(16) Kosa, M.; Karni, M.; Apeloig, Y. How to Design Linear Allenic-Type Trisilaallenes and Trigermaallenes. *J. Am. Chem. Soc.* **2004**, *126*, 10544−10545.

(17) Sun, G.; Lucas, M.; Song, Y.; Zhang, J.; Brazier, C.; Houston, P. L.; Bowman, J. M. H atom Product Channels in the Ultraviolet Photodissociation of the 2-Propenyl Radical. *J. Phys. Chem. A* **2019**, *123*, 9957−9965.

(18) Xu, W.; Yang, J.; Xiao, W. The Silicon Hydride Clusters Si_3H_n ($n \leq 8$) and Their Anions: Structures, Thermochemistry, and Electron Affinities. *J. Phys. Chem. A* **2004**, *108*, 11345−11353.

(19) Burcat, A.; Goos, E. Ideal Gas Thermochemical Properties of Silicon Containing Inorganic, Organic Compounds, Radicals, Andions. *Int. J. Chem. Kinet.* **2018**, *50*, 633−650.

(20) Gámez, J. A.; Hermann, M.; Frenking, G. Structures and Bonding Situation of the Allyl Systems and Cyclic Isomers [H_2E−E(H)−EH_2]$^{-,0,+}$ (E = C, Si, Ge, Sn). *Z. Anorg. Allg. Chem.* **2013**, *639*, 2493−2501.

(21) Vernon, M. F. *Molecular-Beam Scattering*. Ph.D. Thesis, University of California: Berkeley, CA, 1983.

(22) Weiss, P. S. *Reaction Dynamics of Electronically Excited Alkali Atoms with Simple Molecules*. Ph.D. Thesis, University of California, Berkeley, CA, 1986.

(23) Gu, X.; Guo, Y.; Zhang, F.; Mebel, A. M.; Kaiser, R. I. Reaction dynamics of carbon-bearing radicals in circumstellar envelopes of carbon stars. *Faraday Discuss.* **2006**, *133*, 245−275.

(24) Kaiser, R. I.; Ochsenfeld, C.; Stranges, D.; Head-Gordon, M.; Lee, Y. T. Combined crossed molecular beams and *ab initio* investigation of the formation of carbon-bearing molecules in the interstellar medium via neutral-neutral reactions. *Faraday Discuss.* **1998**, *109*, 183−204.

(25) Levine, R. D. *Molecular Reaction Dynamics*; Cambridge University Press, 2005.

(26) Ribeiro, J. M.; Mebel, A. M. Reaction Mechanism and Product Branching Ratios of the CH + C_3H_4 Reactions: A Theoretical Study. *Phys. Chem. Chem. Phys.* **2017**, *19*, 14543−14554.

(27) Miller, W. B.; Safron, S. A.; Herschbach, D. R. Exchange Reactions of Alkali Atoms with Alkali Halides: a Collision Complex Mechanism. *Discuss. Faraday Soc.* **1967**, *44*, 108−122.

(28) Peterson, K. A.; Woon, D. E.; Dunning, T. H. Benchmark Calculations with Correlated Molecular Wave Functions. IV. The Classical Barrier Height of the H+H_2 →H_2+H Reaction. *J. Chem. Phys.* **1994**, *100*, 7410−7415.

(29) Kaiser, R. I.; Maksyutenko, P.; Ennis, C.; Zhang, F.; Gu, X.; Krishtal, S. P.; Mebel, A. M.; Kostko, O.; Ahmed, M. Untangling the Chemical Evolution of Titan's Atmosphere and Surface−from Homogeneous to Heterogeneous Chemistry. *Faraday Discuss.* **2010**, *147*, 429−478.

(30) Becke, A. D. Density-functional Thermochemistry. III. The Role of Exact Exchange. *J. Chem. Phys.* **1993**, *98*, 5648−5652.

(31) Lee, C.; Yang, W.; Parr, R. G. Development of the Colle-Salvetti Correlation-energy Formula into a Functional of the Electron Density. *Phys. Rev. B: Condens. Matter Mater. Phys.* **1988**, *37*, 785−789.

(32) Dunning, T. H., Jr. Gaussian Basis Sets for use in Correlated Molecular Calculations. I. The Atoms Boron Through Neon and Hydrogen. *J. Chem. Phys.* **1989**, *90*, 1007−1023.

(33) Grimme, S. Semiempirical Hybrid Density Functional with Perturbative Second-order Correlation. *J. Chem. Phys.* **2006**, *124*, 034108.

(34) Goerigk, L.; Grimme, S. Efficient and Accurate Double-Hybrid-Meta-GGA Density FunctionalssEvaluation with the Extended GMTKN30 Database for General Main Group Thermochemistry, Kinetics, and Noncovalent Interactions. *J. Chem. Theory Comput.* **2011**, *7*, 291−309.

(35) Grimme, S.; Ehrlich, S.; Goerigk, L. Effect of the Damping Function in Dispersion Corrected Density Functional Theory. *J. Comput. Chem.* **2011**, *32*, 1456−1465.

(36) Cížek, J. *Advances in Chemical Physics*; Wiley Interscience: New York, 1969; Vol. *14*.

(37) Purvis, G. D., III; Bartlett, R. J. A Full Coupled-Cluster Singles and Doubles Model: The Inclusion of Disconnected Triples. *J. Chem. Phys.* **1982**, *76*, 1910−1918.

(38) Scuseria, G. E.; Janssen, C. L.; Schaefer, H. F., III An Efficient Reformulation of the Closed-shell Coupled Cluster Single and Double Excitation (CCSD) Equations. *J. Chem. Phys.* **1988**, *89*, 7382−7387.

(39) Scuseria, G. E.; Schaefer, H. F., III Is Coupled Cluster Singles and Doubles (CCSD) More Computationally Intensive than Quadratic Configuration Interaction (QCISD)? *J. Chem. Phys.* **1989**, *90*, 3700−3703.

(40) Adler, T. B.; Knizia, G.; Werner, H.-J. A Simple and Efficient CCSD(T)-F12 Approximation. *J. Chem. Phys.* **2007**, *127*, 221106.

(41) Knizia, G.; Adler, T. B.; Werner, H.-J. Simplified CCSD(T)-F12 Methods: Theory and Benchmarks. *J. Chem. Phys.* **2009**, *130*, 054104.

(42) Werner, H. J.; Knowles, P. J.; Knizia, G.; Manby, F. R.; Schütz, M.; Celani, P.; Györffy, W.; Kats, D.; Korona, T.; Lindh, R.; Mitrushenkov, A.; Rauhut, G.; Shamasundar, K. R.; Adler, T. B.; Amos, R. D.; Bernhardsson, A.; Berning, A.; Cooper, D. L.; Deegan, M. J. O.; Dobbyn, A. J.; Eckert, F.; Goll, E.; Hampel, C.; Hesselmann, A.; Hetzer, G.; Hrenar, T.; Jansen, G.; Köppl, C.; Liu, Y.; Lloyd, A. W.; Mata, R. A.; May, A. J.; McNicholas, S. J.; Meyer, W.; Mura, M. E.; Nicklaß, A.; O'Neill, D. P.; Palmieri, P.; Peng, D.; Pflüger, K.; Pitzer, R.; Reiher, M.; Shiozaki, T.; Stoll, H.; Stone, A. J.; Tarroni, R.; Thorsteinsson, T.; Wang, M. *MOLPRO*, Verson 2010.1, University College Cardiff Consultants Ltd: United Kingdom, 2010.

(43) Martin, J. M. L.; Uzan, O. Basis Set Convergence in Second-row Compounds. The Importance of Core Polarization Functions. *Chem. Phys. Lett.* **1998**, *282*, 16−24.

(44) Hill, J. G.; Mazumder, S.; Peterson, K. A. Correlation Consistent Basis Sets for Molecular Core-valence Effects with Explicitly Correlated Wave Functions: The Atoms B−Ne and Al−Ar. *J. Chem. Phys.* **2010**, *132*, 054108.

(45) Barone, V. Anharmonic Vibrational Properties by a Fully Automated Second-order Perturbative Approach. *J. Chem. Phys.* **2005**, *122*, 014108.

(46) Frisch, M. J.; Trucks, G. W.; Schlegel, H. B.; Scuseria, G. E.; Robb, M. A.; Cheeseman, J. R.; Scalmani, G.; Barone, V.; Mennucci, B.; Petersson, G. A.; Nakatsuji, H.; Caricato, M.; Li, X.; Hratchian, H. P.; Izmaylov, A. F.; Bloino, J.; Zheng, G.; Sonnenberg, J. L.; Hada, M.; Ehara, M.; Toyota, K.; Fukuda, R.; Hasegawa, J.; Ishida, M.; Nakajima, T.; Honda, Y.; Kitao, O.; Nakai, H.; Vreven, T.; Montgomery, J. A., Jr.; Peralta, J. E.; Ogliaro, F.; Bearpark, M.; Heyd, J. J.; Brothers, E.; Kudin, K. N.; Staroverov, V. N.; Kobayashi, R.; Normand, J.; Raghavachari, K.; Rendell, A.; Burant, J. C.; Iyengar, S. S.; Tomasi, J.; Cossi, M.; Rega, N.; Millam, J. M.; Klene, M.; Knox, J. E.; Cross, J. B.; Bakken, V.; Adamo, C.; Jaramillo, J.; Gomperts, R.; Stratmann, R. E.; Yazyev, O.; Austin, A. J.; Cammi, R.; Pomelli, C.; Ochterski, J. W.; Martin, R. L.; Morokuma, K.; Zakrzewski, V. G.; Voth, G. A.; Salvador, P.; Dannenberg, J. J.; Dapprich, S.; Daniels, A. D.; Farkas, O.; Foresman, J. B.; Ortiz, J. V.; Cioslowski, J.; Fox, D. J. *Gaussian 09*, revision D.01; Gaussian, Inc.: Wallingford, CT, 2009.

https://dx.doi.org/10.1021/acs.jpclett.0c02281
J. Phys. Chem. Lett. 2020, 11, 7874−7881